United States Department of Commerce
National Institute of Standards and Technology

NISTIR 3954

NEAR-FIELD AND FAR-FIELD EXCITATION OF A LONG CONDUCTOR IN A LOSSY MEDIUM

David A. Hill

NISTIR 3954

NEAR-FIELD AND FAR-FIELD EXCITATION OF A LONG CONDUCTOR IN A LOSSY MEDIUM

David A. Hill

Electromagnetic Fields Division
Center for Electronics and Electrical Engineering
National Engineering Laboratory
National Institute of Standards and Technology
Boulder, Colorado 80303-3328

September 1990

Sponsored by
U.S. Army Belvoir RD&E Center
Fort Belvoir, Virginia 22060-5606

U.S. DEPARTMENT OF COMMERCE, Robert A. Mosbacher, Secretary
NATIONAL INSTITUTE OF STANDARDS AND TECHNOLOGY, John W. Lyons, Director

NEAR-FIELD AND FAR-FIELD EXCITATION OF A LONG CONDUCTOR IN A LOSSY MEDIUM

David A. Hill

Electromagnetic Fields Division
National Institute of Standards and Technology
Boulder, CO 80303

Excitation of currents on an infinitely long conductor is analyzed for horizontal electric dipole or line sources and for a plane-wave, far-field source. Any of these sources can excite strong currents which produce strong scattered fields for detection. Numerical results for these sources indicate that long conductors produce a strong anomaly over a broad frequency range. The conductor can be either insulated or bare to model ungrounded or grounded conductors.

Key words: axial current; axial impedance; electric dipole; electric field; grounded conductor; insulated conductor; line source; magnetic field; plane wave.

1. INTRODUCTION

The excitation of currents on long, underground conductors is important in many applications. Power lines and rails in tunnels can enhance transmission for mine communication [1]. Cables or pipes can influence electromagnetic probing of the earth [2].

In this report, we examine the feasibility of electromagnetic detection of long conductors in tunnels. This approach differs from the usual tunnel detection techniques that attempt to detect an air-filled cavity using VHF frequencies and vertical electric field polarization [3,4]. For strong excitation of currents on long, horizontal conductors, we consider the use of lower frequencies and horizontal polarization [5].

Our model consists of an infinitely long conductor that can be bare or insulated in a homogeneous, lossy earth. In section 2, we consider near-field excitation with a horizontal electric dipole source; the analysis parallels an earlier study of vertical magnetic dipole excitation [6]. The extension to near-field excitation with an electric line source of finite length is covered in section 3. In section 4, we consider far-field

excitation with a plane-wave source. In all cases, we assume that the conductor is at a sufficient depth that we do not need to consider air-earth interface effects [7-9], and we neglect the effect of the air-earth interface on the excitation fields. The model is idealized, but it allows us to consider most of the relevant features of the practical problem.

2. HORIZONTAL ELECTRIC DIPOLE EXCITATION

2.1 Formulation

The geometry is shown in figure 1. An infinitely long conductor of outer radius b is centered on the z-axis. A short horizontal (z-directed) electric dipole of current moment IL is located at (x_d, y_d, z_d). The earth has permittivity ϵ, conductivity σ, and magnetic permeability μ.

The formulation for the fields of the dipole source and the infinitely long conductor closely follows [6]. The fields due to the electric dipole in the absence of the conductor can be derived from an electric Hertz vector with only a z component Π_z^d. For $\exp(j\omega t)$ time dependence, Π_z^d is

$$\Pi_z^d = \frac{IL}{4\pi(\sigma + j\omega\epsilon)} \frac{e^{-jkr_d}}{r_d}, \tag{1}$$

where

$$r_d = [(x-x_d)^2 + (y-y_d)^2 + (z-z_d)^2]^{1/2}$$

and

$$k = \omega[\mu(\epsilon - j\sigma/\omega)]^{1/2}.$$

The electric and magnetic fields, $\mathbf{E}^d$ and $\mathbf{H}^d$, due to the dipole are

$$\mathbf{E}^d = (\nabla\nabla\cdot + k^2)(\mathbf{e}_z\Pi_z^d)$$

and (2)

$$H^d = (\sigma + j\omega\epsilon)\ \nabla\times(e_z \Pi_z^d),$$

where e_z is a unit vector in the z direction.

The current on the infinitely long conductor is determined by applying an axial impedance condition in the transform domain. The transform of the current $\hat{I}(\lambda)$ is given by equation (A4) in [6]:

$$\hat{I}(\lambda) = -\frac{IL}{2\pi}\frac{K_0(v\rho_{d0})}{D(\lambda)} e^{j\lambda z_d}, \tag{3}$$

where

$$v = (\lambda^2 - k^2)^{1/2},\ \rho_{d0} = (x_d^2 + y_d^2)^{1/2},$$

$$D(\lambda) = K_0(vb) + \frac{2\pi(\sigma + j\omega\epsilon)}{v^2} Z_s(\lambda),$$

λ is a spatial transform variable, and K_0 is the zero-order modified Bessel function of the second kind [10]. The square root is taken so that the real part of v is positive. $Z_s(\lambda)$ is the axial impedance (series impedance per unit length) of the conductor.

A useful model for a buried insulated conductor is shown in figure 2. It consists of a metal center conductor of radius a surrounded by an insulating region of outer radius b. The metal has conductivity σ_m and magnetic permeability μ_m, and the insulation has permittivity ϵ_i and free space permeability μ_0. The axial impedance of this model is [8,11]

$$Z_s(\lambda) = Z_m + \frac{\lambda^2 - k_i^2}{2\pi j\omega\epsilon_i} \ell n(b/a), \tag{4}$$

where

$$Z_m = \frac{(j\omega\mu_m/\sigma_m)^{1/2}}{2\pi a} \frac{I_0(jk_m a)}{I_1(jk_m a)},$$

$$k_i = \omega(\mu_0\epsilon_i)^{1/2}, \quad jk_m = (j\omega\mu_m\sigma_m)^{1/2},$$

and I_0 and I_1 are modified Bessel functions of the first kind [10]. If we set $b = a$, then $Z_s(\lambda) = Z_m$, and we have a grounded conductor (such as a rail in a tunnel). If we set ϵ_i equal to the free-space permittivity ϵ_0, then we can model a conductor (such as a power line) suspended in an air-filled tunnel at a distance b - a from the tunnel wall.

2.2 Conductor Current

The current I(z) on the conductor is given as an inverse transform [6]

$$I(z) = \int_{-\infty}^{\infty} \hat{I}(\lambda)\, e^{-j\lambda z}\, d\lambda, \tag{5}$$

where $\hat{I}(\lambda)$ is the transform current given in (3). $\hat{I}(\lambda)$ has branch points at $\lambda = \pm k$ and poles at $\lambda = \pm \lambda_p$, where λ_p is determined by

$$D(\lambda_p) = 0. \tag{6}$$

The numerical solution of (6) is discussed in [6]. The pole contribution $I_p(z)$ to the integral in (5) is

$$I_p(z) = jIL \left[\frac{K_0(v\rho_{d0})}{D'(\lambda)}\right]\Bigg|_{\lambda=\lambda_p} e^{-j\lambda_p|z-z_d|}, \tag{7}$$

where $D'(\lambda) = \frac{\partial D}{\partial \lambda}$.

The pole contribution in (7) is called the transmission line current or quasi-TEM current. It exists only for b > a.

The integral for the total conductor current I(z) in (5) is most easily evaluated by fast Fourier transform (FFT), and this method automatically yields an array of z values. Numerical results for the magnitude of I(z) are shown in figure 3 for the following parameters: IL = 1 A•m, x_d = 15 m, y_d = 50 m, z_d = 0, f = 20 kHz, $\sigma_m = 5.7 \times 10^7$ S/m, $\mu_m = \mu = \mu_0$, a = 0.5 cm, $\epsilon_i = \epsilon_0$, $\epsilon/\epsilon_0 = 10$, and $\sigma = 5 \times 10^{-3}$ S/m. The currents are even in z. The currents on the insulated conductor (b > a) have a slow z decay because of the dominance of the transmission line current as given by (7). These currents actually differ very little from $I_p(z)$ as given by (7). The current on the bare (grounded) conductor has a higher peak value, but has rapid exp(-jk|z|) decay corresponding to plane wave attenuation in the earth.

2.3 Magnetic Field

In this section, we consider the primary magnetic field due to the dipole and the secondary magnetic field due to the conductor. The y-component of the magnetic field is of most interest because we anticipate reception with a vertical magnetic dipole in a vertical borehole.

The primary y-component H_y^d of the magnetic field due to the electric dipole source is obtained by substituting (1) into (2):

$$H_y^d = -(\sigma + j\omega\epsilon) \frac{\partial \Pi_z^d}{\partial x} \tag{8}$$

$$= \frac{IL}{4\pi} \left(\frac{x - x_d}{r_d}\right) \left(jk + \frac{1}{r_d}\right) \frac{e^{-jkr_d}}{r_d}.$$

In general both the jk and the $1/r_d$ terms in (8) must be retained.

The secondary y-component H_y^c due to the conductor is [6]

$$H_y^c = \frac{x}{2\pi\rho} \int_{-\infty}^{\infty} \hat{I}(\lambda)\, vK_1(v\rho)\, e^{-j\lambda z}, \tag{9}$$

where

$$\rho = (x^2 + y^2)^{1/2}$$

and $\hat{I}(\lambda)$ is given by (3). In general we choose to evaluate the integral in (9) by FFT. However, the pole contribution $H_{yp}^c(z)$ for the case of the insulated conductor is given by [6]

$$H_{yp}^c(z) = \left[\frac{xvK_1(v\rho)}{2\pi\rho}\right]\Bigg|_{\lambda=\lambda_p} I_p(z), \tag{10}$$

where $I_p(z)$ is given by (7).

In figure 4 we show the primary and secondary magnetic field strengths observed at x = 15 m and y = 0 for the same parameters as used in figure 3. The magnetic field due to an insulated conductor decays slowly in z because it is dominated by the pole contribution given by (10). For large z, the secondary magnetic field is larger than the primary field, and the insulated conductor should be detectable. The secondary field for a grounded conductor has a more rapid decay, but it still exceeds the primary field for large z. These results are qualitatively the same as those for a magnetic dipole source in [6].

In figure 5 we show the magnetic field results for three values of x, and these results are relevant to reception at different horizontal separations (ranges). The insulation radius b is 1 cm, and the other parameters are the same as in figures 3 and 4. Even though the magnetic fields decrease for increasing x, the secondary field exceeds the primary field for large values of z.

In figure 6 we show the magnetic field results for different frequencies from 4 kHz to 500 kHz for x = 15 m. The other parameters are

the same as those in figure 5. In all cases the secondary magnetic field exceeds the primary field for large z. The largest secondary magnetic field is obtained for a frequency of 20 kHz. These results apply to infinitely long conductors; for conductors of finite length [12] the optimum frequency could be higher.

2.4 Electric Field

The infinitely long conductor also produces a strong secondary electric field which could be received with a horizontal electric dipole. We consider the z-component of the primary and secondary electric fields because this is the strongest component.

The primary z-component E_z^d of the electric field due to the electric dipole source is obtained by substituting (1) into (2):

$$E_z^d = \left(\frac{\partial^2}{\partial z^2} + k^2\right) \Pi_z^d \tag{11}$$

$$= \frac{IL\, e^{-jkr_d}}{4\pi r_d(\sigma + j\omega\epsilon)} \left\{k^2\left[1 - \frac{(z-z_d)^2}{r_d^2}\right] + \right.$$

$$\left. + \frac{jk}{r_d}\left[\frac{3(z-z_d)^2}{r_d^2} - 1\right] + \frac{1}{r_d^2}\left[\frac{3(z-z_d^2)}{r_d^2} - 1\right]\right\}.$$

In general all terms in (8) must be retained.

The secondary z-component E_z^c due to the conductor is [6]

$$E_z^c = \frac{-1}{2\pi(\sigma + j\omega\epsilon)} \int_{-\infty}^{\infty} \hat{I}(\lambda) v^2 K_0(v\rho)\, e^{-j\lambda z}\, d\lambda, \tag{12}$$

where $\hat{I}(\lambda)$ is given by (3). In general we choose to evaluate the integral in (12) by FFT. However, the pole contribution $E^c_{zp}(z)$ for the case of the insulated conductor is given by

$$E^c_{zp}(z) = \left[\frac{-v^2 K_0(v\rho)}{2\pi(\sigma + j\omega\epsilon)}\right]\Bigg|_{\lambda=\lambda_p} I_p(\lambda), \tag{13}$$

where $I_p(z)$ is given by (7).

In figure 7 we show the primary and secondary electric field strengths for the same parameters as used in figure 4. The electric field due to an insulated conductor decays slowly in z because it is dominated by the pole contribution given by (13). For large z, the secondary electric field is larger than the primary field, and the insulated conductor should be detectable. The secondary field for a grounded conductor has a higher peak, but has a more rapid decay. These results are qualitively the same as those for the magnetic field in figure 4.

In figure 8 we show electric field results for the same parameters as used in figure 5, and the various values of x are relevant to reception at different horizontal ranges. The electric fields decrease for increasing x, but the secondary field exceeds the primary field for large values of z. These results are qualitively the same as those for the magnetic field in figure 5.

In figure 9 we show the electric field results for different frequencies for the same parameters as those in figure 6. In all cases the secondary field exceeds the primary field for large z. The largest secondary field is obtained for a frequency of 100 kHz.

3. LINE SOURCE EXCITATION

In this section we consider the case where the source is a horizontal line current of finite length. This extension is of practical importance because a long insulated wire grounded at both ends is a commonly used

antenna for producing a horizontally polarized electric field [5]. The antenna could be located either at the earth surface [13] or underground [14]. Since we neglect the air-earth interface in this analysis, the line current is located in a homogeneous medium.

3.1 Formulation

The geometry shown in figure 10 is the same as that in figure 1 except that the dipole source is replaced by a horizontal (z-directed) electric current line source. The line source of length L is centered at (x_d, y_d, z_d) and carries a constant current I.

The z-component of the electric Hertz vector can be obtained by integrating the short dipole result in (1) over the length of the line source:

$$\Pi_z^d = \frac{I}{4\pi(\sigma + j\omega\epsilon)} \int_{z_d-\frac{L}{2}}^{z_d+\frac{L}{2}} \frac{e^{-jkr'_d}}{r'_d}\, dz', \tag{14}$$

where

$$r'_d = [(x-x_d)^2 + (y-y_d)^2 + (z-z')^2]^{1/2}.$$

The primary fields of the line source are obtained by substituting (14) into (2).

To determine the current induced on the infinitely long conductor, we follow the method in [6]. The exponential in (14) can be written in integral form [15], and Π_z^d in (14) becomes

$$\Pi_z^d = \frac{I}{4\pi^2(\sigma + j\omega\epsilon)} \int_{z_d-\frac{L}{2}}^{z_d+\frac{L}{2}} \int_{-\infty}^{\infty} K_0(v\rho_d)\, e^{-j\lambda(z-z')}\, d\lambda\, dz', \tag{15}$$

where

$$\rho_d = [(x-x_d)^2 + (y-y_d)^2]^{1/2}.$$

If we reverse the order of integration in (15), the z′ integration can be performed to yield

$$\Pi_z^d = \frac{IL}{4\pi^2(\sigma + j\omega\epsilon)} \int_{-\infty}^{\infty} K_0(v\rho_d) \frac{\sin(\lambda L/2)}{(\lambda L/2)} e^{-j\lambda(z-z_d)} d\lambda. \qquad (16)$$

When L approaches zero in (16), the factor $\sin(\lambda L/2)/(\lambda L/2)$ approaches one, and (16) reduces to the result for a short dipole.

3.2 Conductor Current

The transform of the conductor current is the same as given by (3) for the short dipole source except that a factor $\sin(\lambda L/2)/(\lambda L/2)$ is introduced to account for the length of the line source:

$$\hat{I}(\lambda) = -\frac{IL}{2\pi} \frac{K_0(v\rho_{d0})}{D(\lambda)} \frac{\sin(\lambda L/2)}{(\lambda L/2)} e^{j\lambda z_d}. \qquad (16)$$

The current I(z) on the conductor is obtained by substituting (16) into the inverse transform in (5).

For insulated conductors (b > a), the current is approximately equal to the pole contribution. Beyond the ends of the line source ($|z - z_p| > L/2$), the pole contribution $I_p(z)$ to the current is

$$I_p(z) = jIL \left[\frac{K_0(v\rho_{d0})}{D'(\lambda)} \frac{\sin(\lambda L/2)}{(\lambda L/2)}\right]\Bigg|_{\lambda=\lambda_p} e^{-j\lambda_p|z-z_d|}. \qquad (17)$$

For convenience in studying the effect of source length L on the conductor current, we define the following ratio R(L):

$$R(L) = \frac{I_p(z)}{I_p(z)\big|_{L = 1\ m}}, \tag{18}$$

where $I_p(z)$ is given by (17). For the frequencies of interest here (< 500 kHz), R(L) is approximately given by

$$R(L) \approx L \frac{\sin(\lambda_p L/2)}{(\lambda_p L/2)}, \tag{19}$$

where λ_p is determined from the mode equation (6) and L is given in m. Numerical results for the magnitude of R are shown in figure 11 for frequencies of 20 and 100 kHz and b = 1 cm. The remaining conductor and earth parameters are the same as in figure 3. For small L, |R| is proportional to L as is the induced current for a dipole source in (7). For larger L, phase cancellation begins to occur, and a maximum in |R| occurs near $L \approx \pi/\mathrm{Re}(\lambda_p)$, where Re indicates the real part. From figure 11, the first maximum in |R| occurs at L ≈ 450 m for a frequency of 100 kHz. If L is made too long, the assumption of constant source current is no longer valid.

4. PLANE WAVE EXCITATION

When the source is located a great distance, the incident field can be considered to be a plane wave. For example, a distant VLF station at a frequency of 17.4 kHz has been found to be a useful source [5]. Since we are considering low frequencies, the refractive index of the earth is large, and the incident field is refracted normal to the earth surface. Thus the incident field propagates vertically downward in the negative y direction as shown in figure 12. The infinitely long conductor is the same as shown in figures 1 and 2.

Of the two possible electric field polarizations of the electric field (x and z), only z polarization induces axial currents in the long z-directed

conductor. So we assume that the incident electric field has only a z-component E_z^i given by

$$E_z^i = E_0 \, e^{jky}, \tag{20}$$

where k is given by (1). The incident magnetic field has only an x-component H_x^i given by

$$H_x^i = - H_0 \, e^{jky}, \tag{21}$$

where $H_0 = E_0/\eta$ and the intrinsic impedance $\eta = [\mu/(\epsilon - j\sigma/\omega)]^{1/2}$.

4.1 Conductor Current

For uniform field excitation, the conductor current I is a constant independent of z. To determine I, we apply the axial impedance condition that was used in [6] for the special case of a uniform field ($\lambda = 0$):

$$(E_z^i + E_z^c)\big|_{y=0,\ x=b} = IZ_{s0}. \tag{22}$$

Z_{s0} is obtained by setting $\lambda = 0$ in Z_s in (4):

$$Z_{s0} = Z_m + \frac{j\omega\mu_0}{2\pi} \ell n(b/a). \tag{23}$$

The z-component E_z^c of the electric field due to the conductor is

$$E_z^c = \frac{-j\omega\mu I}{2\pi} K_0(jk\rho). \tag{24}$$

If we substitute (23) and (24) into (22) and set $\mu = \mu_0$, we obtain the following for I:

$$I = \frac{E_0}{Z_{s0} + (j\omega\mu_0/2\pi)K_0(jkb)}. \tag{25}$$

A numerical evaluation of (25) indicated that the current I is independent of the outer radius b of the insulation. The reason for this is that for small |kb| the modified Bessel function can be approximated by [10]

$$K_0(jkb) \approx - \ell n(jkb). \tag{26}$$

If we substitute (26) into (25) and perform some algebra, we obtain

$$I \approx \frac{E_0}{Z_m - (j\omega\mu_0/2\pi)\ \ell n(jka)}. \tag{27}$$

This result is very different from the case of dipole excitation where the insulation plays an important role in supporting a transmission line mode. For uniform field excitation, the transmission line mode is not excited.

Numerical results for the magnitude of the current as a function of frequency are shown in figure 13. The results depend on the metal radius a, but not on the insulation radius b. The constitutive parameters of the metal and the earth are the same as in the previous figures. The current increases as the frequency is decreased, but the low-frequency limit of I is a constant. This constant is obtained by letting ω approach zero in Z_m:

$$Z_m\big|_{\omega = 0} = 1/(\pi a^2 \sigma_m). \tag{28}$$

This is the expected dc limit. If we substitute (28) into (27), we obtain the dc limit of I:

$$I\big|_{\omega = 0} = E_0 \, (\pi a^2 \sigma_m). \tag{29}$$

4.2 Electric and Magnetic Fields

The electric field due to the conductor current is given by (24). From Maxwell's curl equation, the x and y components, H_x^c and H_y^c, of the magnetic field due to the conductor current are

$$H_x^c = \frac{-1}{j\omega\mu} \frac{\partial E_z^c}{\partial y} = \frac{-jkIy}{2\pi\rho} K_1(jk\rho)$$

and (30)

$$H_y^c = \frac{1}{j\omega\mu} \frac{\partial E_z^c}{\partial x} = \frac{jkIx}{2\pi\rho} K_1(jk\rho).$$

The vertical component H_y^c is of most practical interest because it is most easily received in a vertical borehole and because it is orthogonal to the incident magnetic field.

In figure 14 we show numerical results for the magnitude of the vertical magnetic field as a function of height y for a number of frequencies. The horizontal distance x is 15 m, and the conductor radius a is 0.5 cm. The other parameters are the same as in figure 13. The field peaks at y = 0 and is even in y. The largest response is at the lowest frequency, 4 kHz, because the induced current is largest at the lowest frequency. Under ideal circumstances, the conductor should be detectable from the maximum in $|H_y^c|$ because the incident field has no vertical component. However, irregularities in the earth and in the earth surface will generally cause some conversion from horizontal to vertical magnetic field [16].

In figure 15 we show numerical results for the magnitude of the vertical magnetic field for various horizontal distances x at a frequency of 20 kHz. The remaining parameters are the same as in figure 14. For larger

offsets of 50 and 100 m, the field strengths are lower and the peak at y = 0 is not very sharp. So detection and location would be difficult.

In figure 16 we show numerical results for $|E_z^c|$ as a function of y for various frequencies. The parameters are the same as those in figure 14. Since the polarization is the same as the incident field and is only on the order of 10% of the incident field, the secondary electric field is probably not very useful for detection.

5. CONCLUSIONS

The results presented here indicate that a horizontal electric dipole can excite significant axial currents on long horizontal conductors. These currents produce secondary magnetic and electric fields that are smaller than the primary fields near the source, but are larger than the primary fields at large axial distances. An insulated conductor can support a transmission line current that has slow decay in the axial direction . A grounded conductor has a larger current excited near the source, but that current decays more rapidly in the axial direction. In either case, the secondary fields are large enough that detection of long conductors appears promising. The same conclusions hold for an electric line source grounded at the ends, and the effect of the length of the line source is discussed in section 3. All of the above conclusions are qualitively the same as those for a magnetic dipole source [6]. Numerical results have been presented for frequencies from 4 kHz to 500 kHz, and the entire frequency range appears to be useful.

If a controlled source is not available, then distant far-field sources, such as VLF radio stations or atmospheric noise, can also be used. Such sources will excite long conductors if the polarization of the electric field is aligned along the conductor, but will not excite a transmission line current. The secondary vertical magnetic field is the most useful field component to use in detection because the incident magnetic field in the earth should be horizontally polarized.

A number of extensions to this work would be useful. The presence of the air-earth interface [9] could be included, and this would be useful in providing a more precise evaluation of excitation by a line source at the earth surface [13]. Multiple conductors or conductors of finite length could be studied, and finite length conductors [12] have been shown to have a significantly different frequency dependence because of resonance effects. Also, earth layering or inhomogeneities could be studied to obtain an estimate of the competing geologic noise [16-19]. This effect could be particularly important in the case of a distant far-field source where polarization is used to discriminate against the incident field.

6. ACKNOWLEDGMENTS

This research was supported by the U.S. Army Belvoir RD&E Center. I would like to thank Roy Greenfield and Larry Stolarczyk for helpful discussions.

7. REFERENCES

[1] Wait, J.R.; Hill, D.A. Radio frequency transmission via a trolley wire in a tunnel with rail return. IEEE Trans. Antennas Propagat., AP-25: 248-253; 1977.

[2] Wait, J.R.; Umashankar, K.R. Analysis of the earth resistivity response of buried cables. Pure and Appl. Geophys., 117: 711-742; 1978.

[3] Lytle, R.J.; Laine, E.F.; Lager, D.L.; Davis, D.T. Cross-borehole electromagnetic probing to locate high-contrast anomalies. Geophys., 44: 1667-1676; 1979.

[4] Olhoeft, G.R. Interpretation of hole-to-hole radar measurements. Third Technical Symposium on Tunnel Detection. Golden, CO: January 12-15, 1988.

[5] Bollen, R.L. Tunnel Detection by Low-Frequency Magnetic-Field Emissions and the Controlled Source Audio Magneto Telluric Techniques. SRI International: January 1989.

[6] Hill, D.A. Magnetic dipole excitation of a long conductor in a lossy medium. IEEE Trans. Geosci. Rem. Sens., GE-26: 720-725; 1988.

[7] Wait, J.R. Electromagnetic wave propagation along a buried insulated wire. Can. J. Phys., 50: 2402-2409; 1972.

[8] Wait, J.R. Excitation of currents on a buried insulated cable. J. Appl. Phys., 49: 876-880; 1978.

[9] Tsubota, K.; Wait, J.R. The frequency and the time-domain responses of a buried axial conductor. Geophys., 45: 941-951; 1980.

[10] Abramowitz, M.; Stegun, I.A. Handbook of Mathematical Functions. Washington: National Bureau of Standards; 1964.

[11] Hill, D.A.; Wait, J.R. Coupling between a dipole antenna and an infinite cable over an ideal ground plane. Radio Sci., 12: 231-238; 1977.

[12] Hill, D.A. Magnetic dipole excitation of an insulated conductor of finite length. IEEE Trans. Geosci. Rem. Sens., GE-28: 289-294; 1990.

[13] Hill, D.A.; Wait, J.R. Subsurface electromagnetic fields of a grounded cable of finite length. Can. J. Phys., 51: 1534-1540; 1973.

[14] Hill, D.A. Electromagnetic surface fields of an inclined buried cable of finite length. J. Appl. Phys., 44: 5275-5279; 1973.

[15] Wait, J.R. Electromagnetic Waves in Stratified Media. New York: Pergamon; 1970.

[16] Hill, D.A.; Wait, J.R. Theoretical noise and propagation models for through-the-earth communication. National Telecommunications and Information Administration; May 1982.

[17] Eaton, P.A.; Hohmann, G.W. An evaluation of electromagnetic methods in the presence of geologic noise. Geophys., 52: 1106-1126; 1987.

[18] Greenfield, R. Borehole radar clutter. National Radio Science Meeting: Boulder, CO; January 4-6, 1989.

[19] Hill, D.A. Clutter models for subsurface electromagnetic applications. Nat. Inst. Stand. Tech. (U.S.) NISTIR 89-3909; 1989.

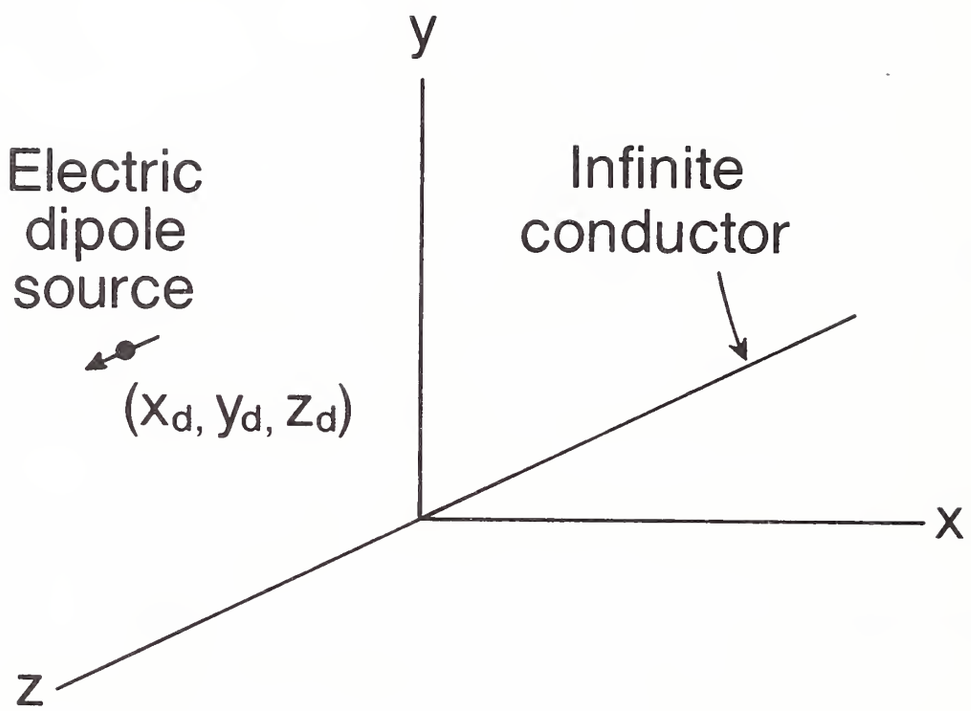

Figure 1. Geometry for a horizontal electric dipole source and an infinitely long conductor.

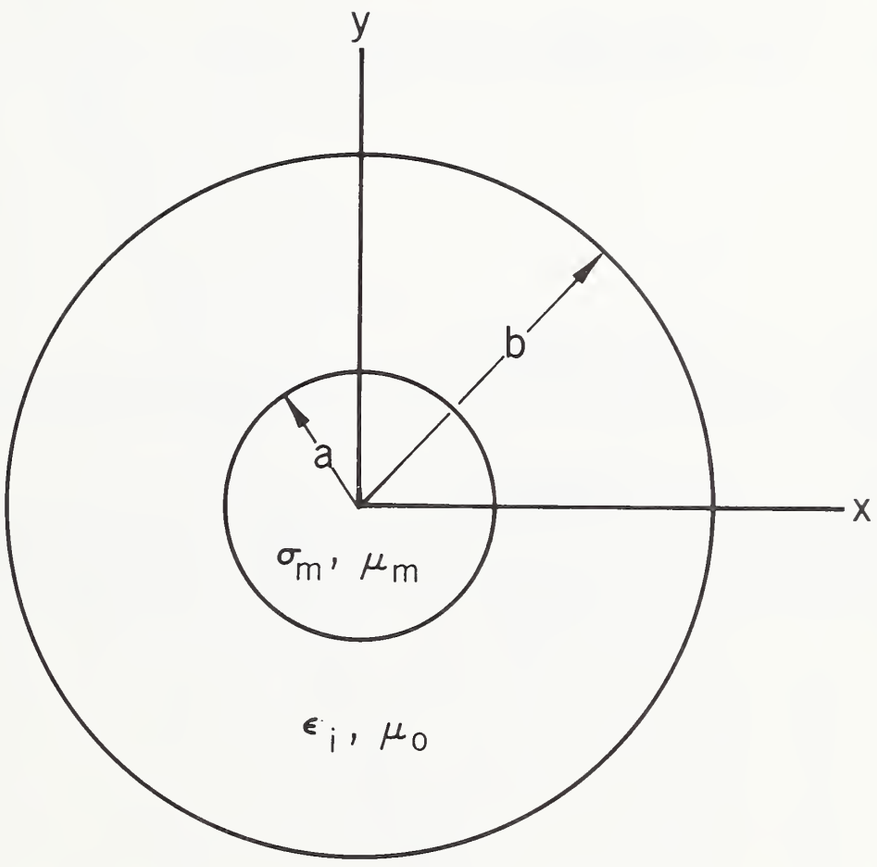

Figure 2. Geometry for an insulated conductor.

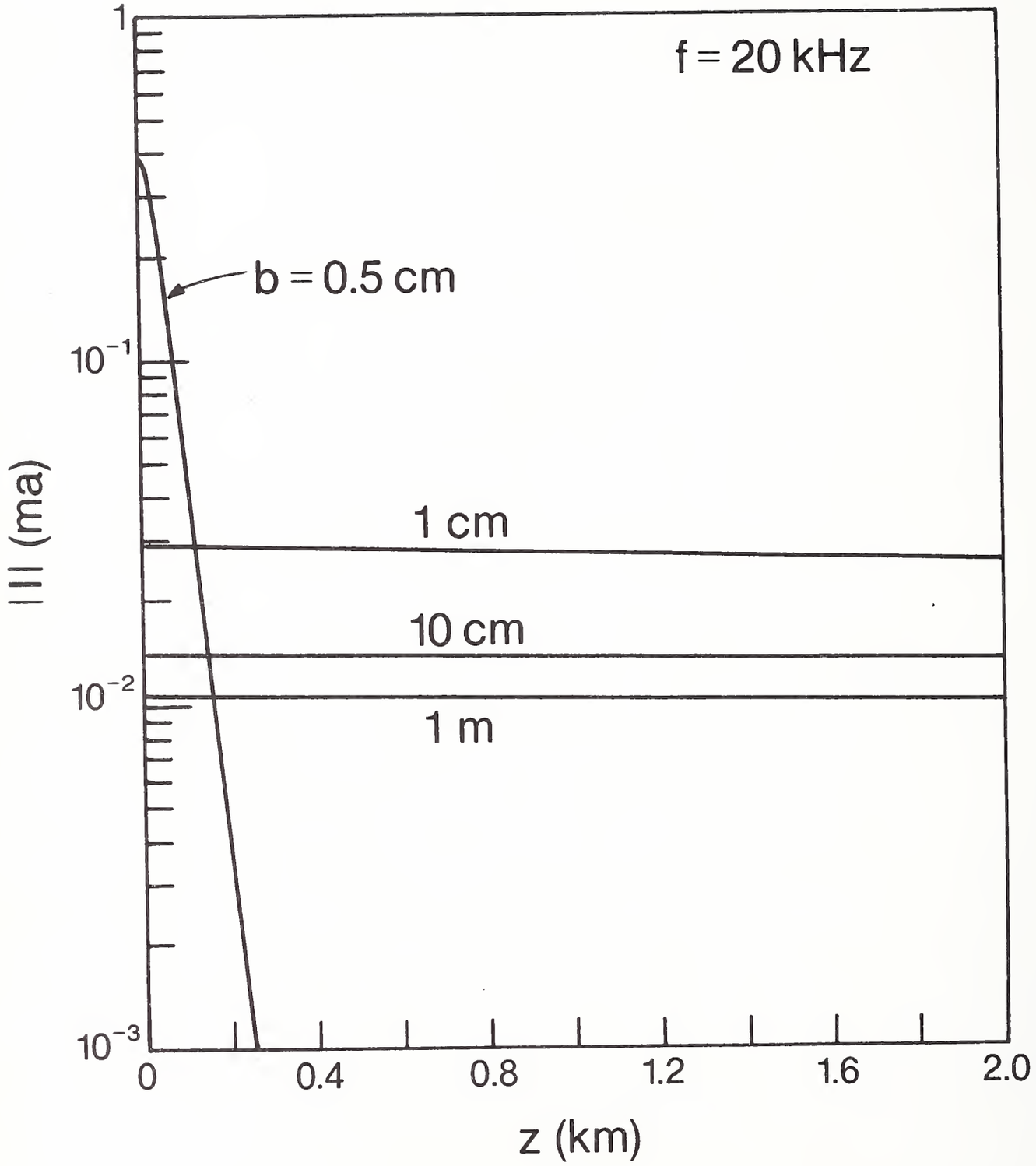

Figure 3. Current induced on a conductor by a horizontal electric dipole source.

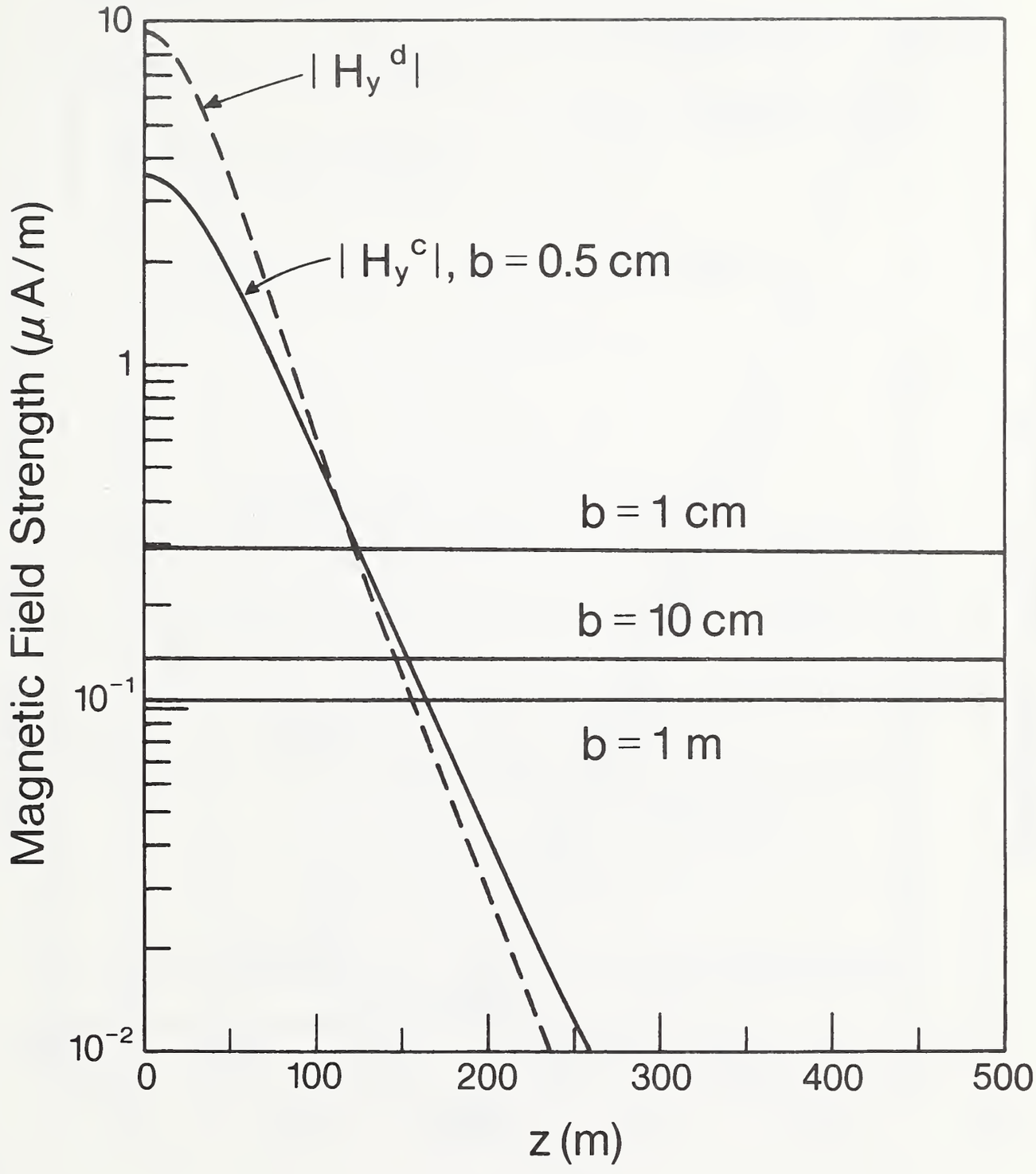

Figure 4. Primary $|H_y^d|$ and secondary $|H_y^c|$ magnetic field strength for different values of insulation radius b.

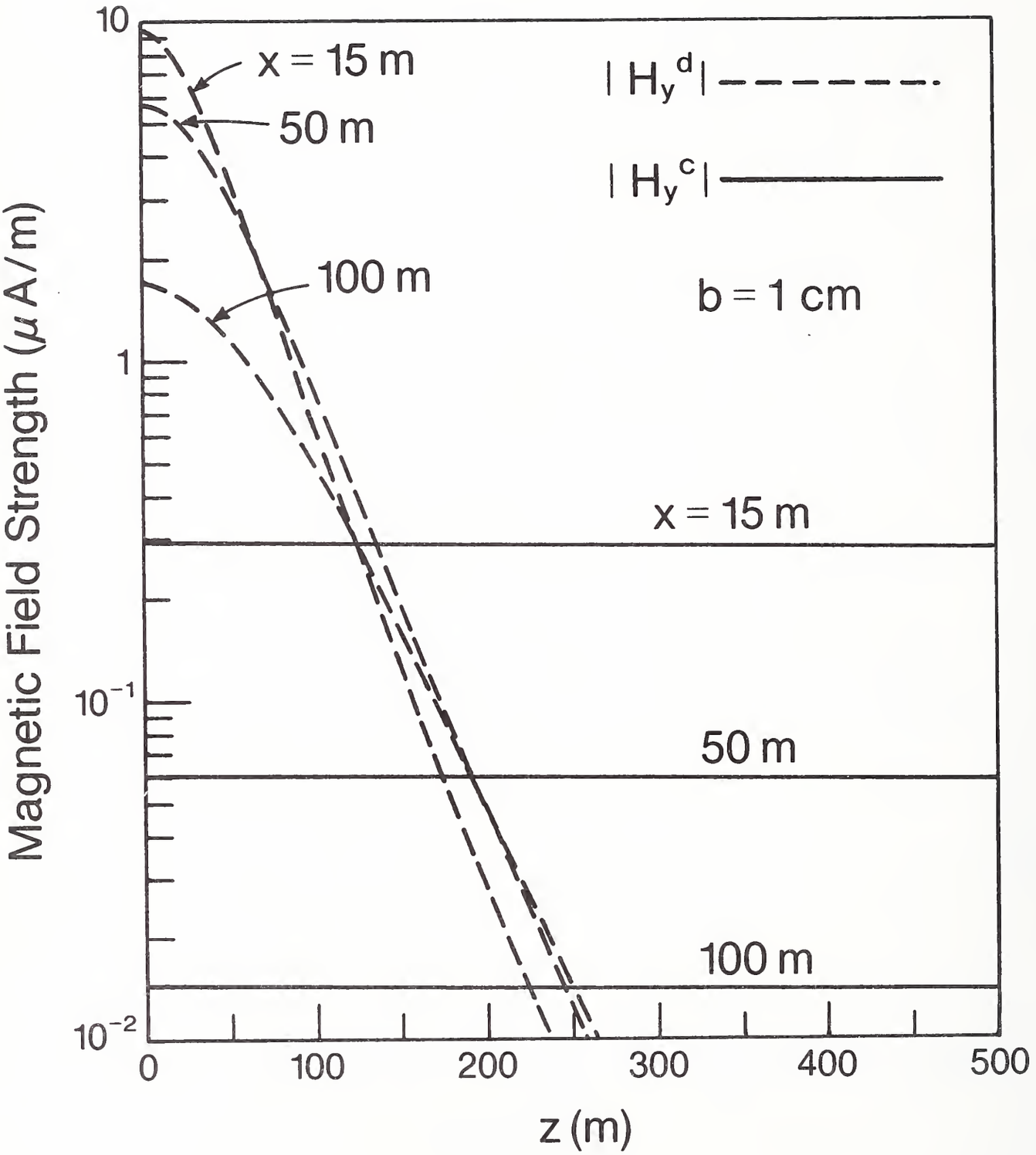

Figure 5. Primary $|H_y^d|$ and secondary $|H_y^c|$ magnetic field strength for different values of horizontal separation x.

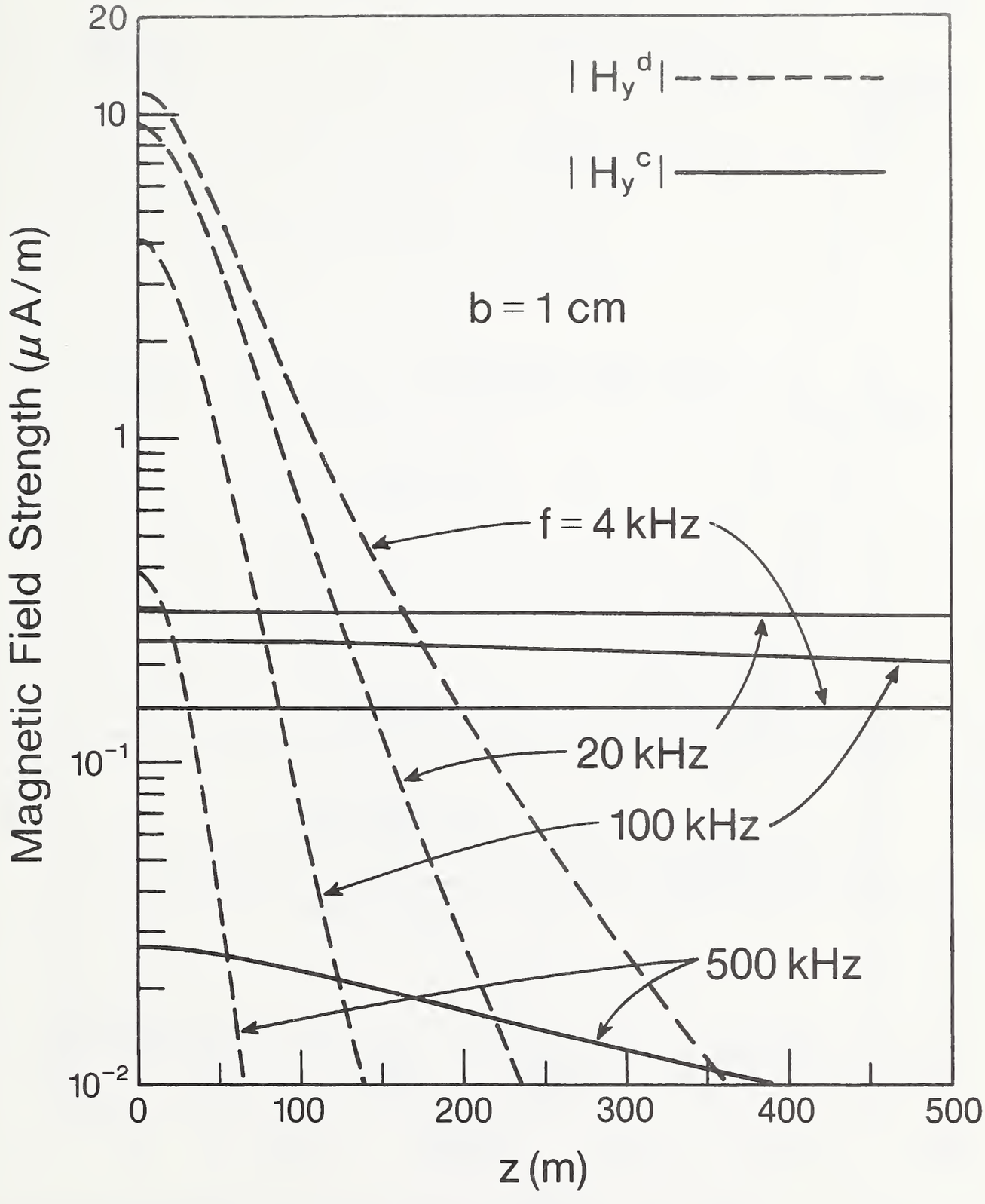

Figure 6. Primary $|H_y^d|$ and secondary $|H_y^c|$ magnetic field strength for different frequencies.

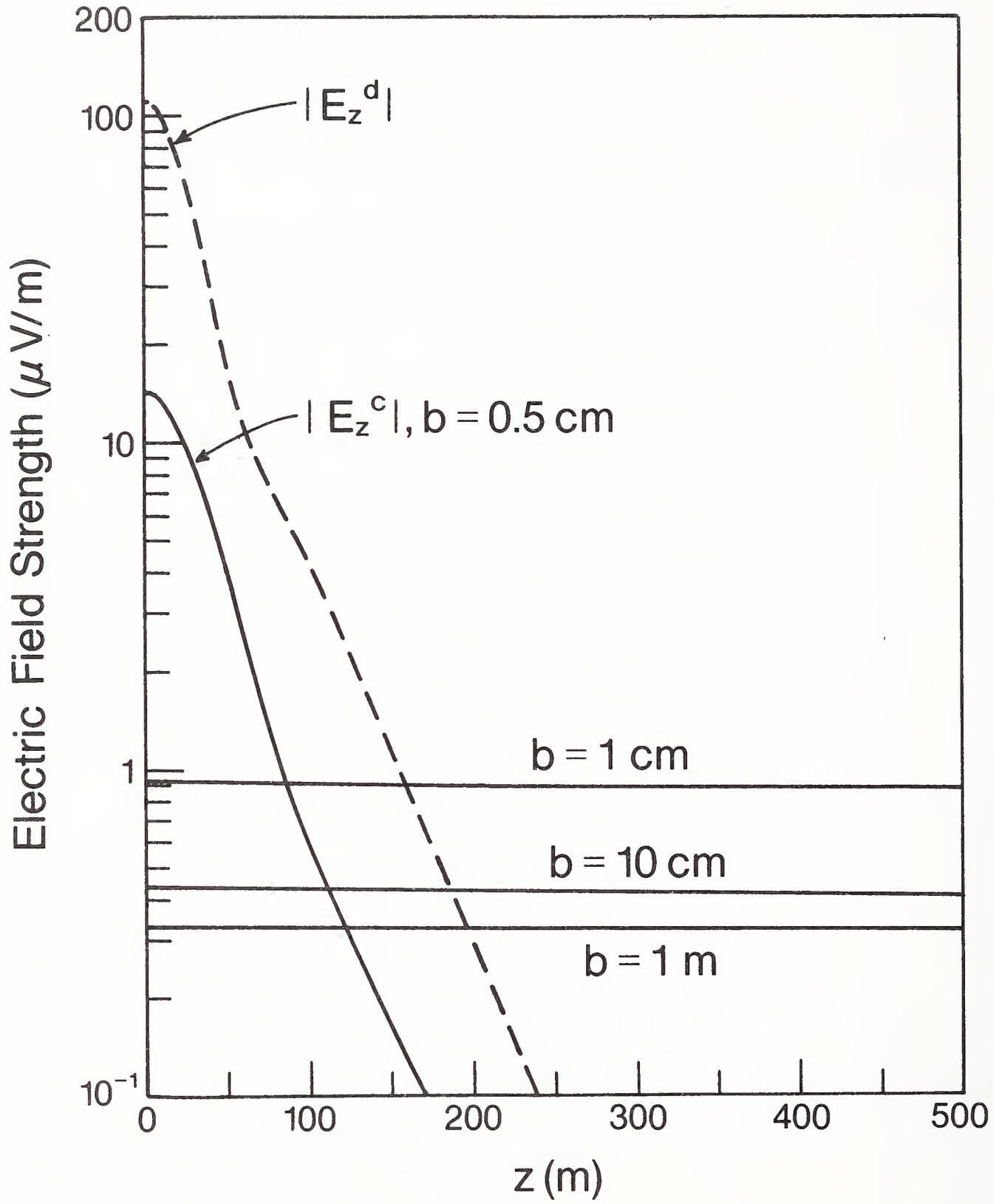

Figure 7. Primary $|E_z^d|$ and secondary $|E_z^c|$ electric field strength for different values of insulation radius b.

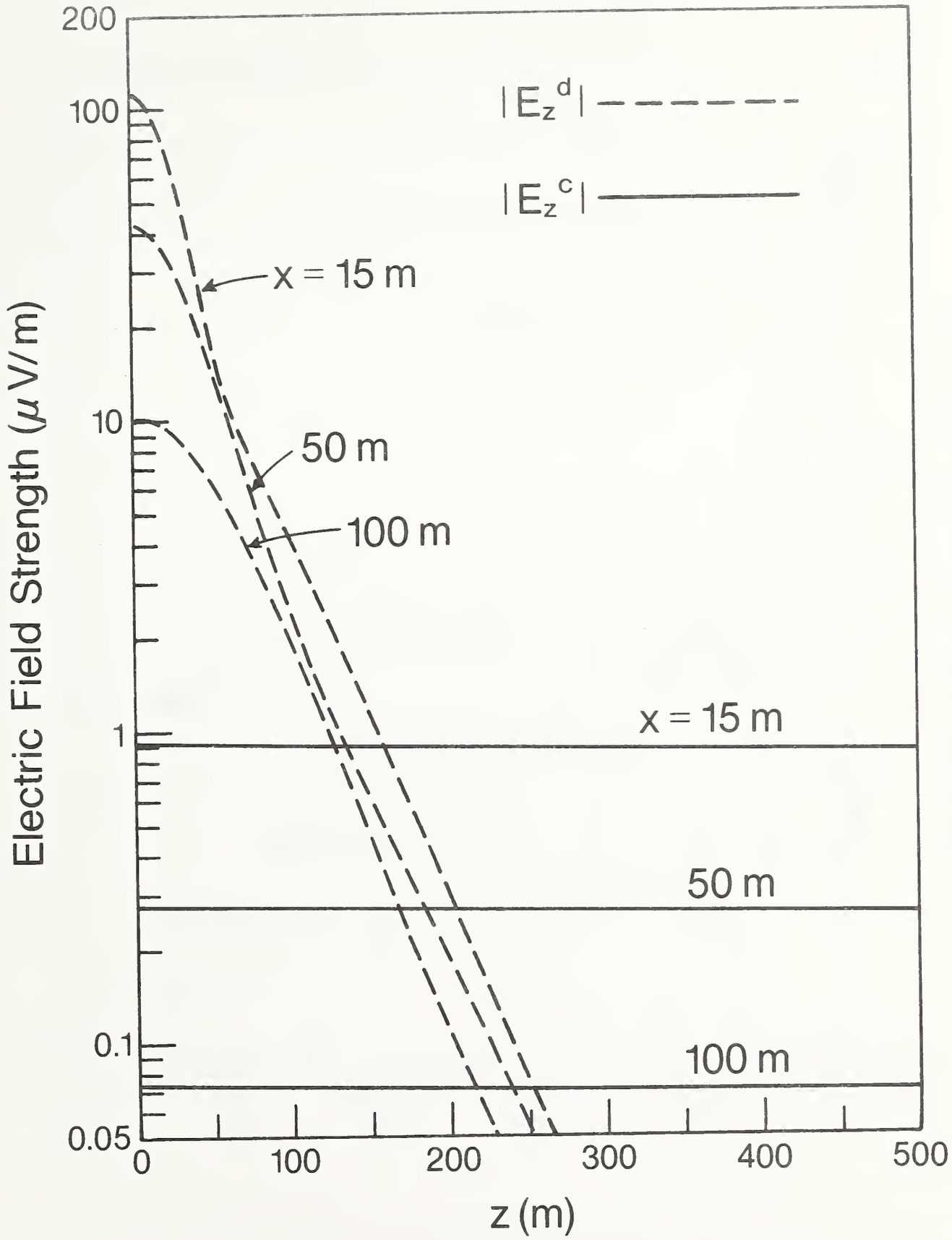

Figure 8. Primary $|E_z^d|$ and secondary $|E_z^c|$ electric field strength for different values of horizontal separation x.

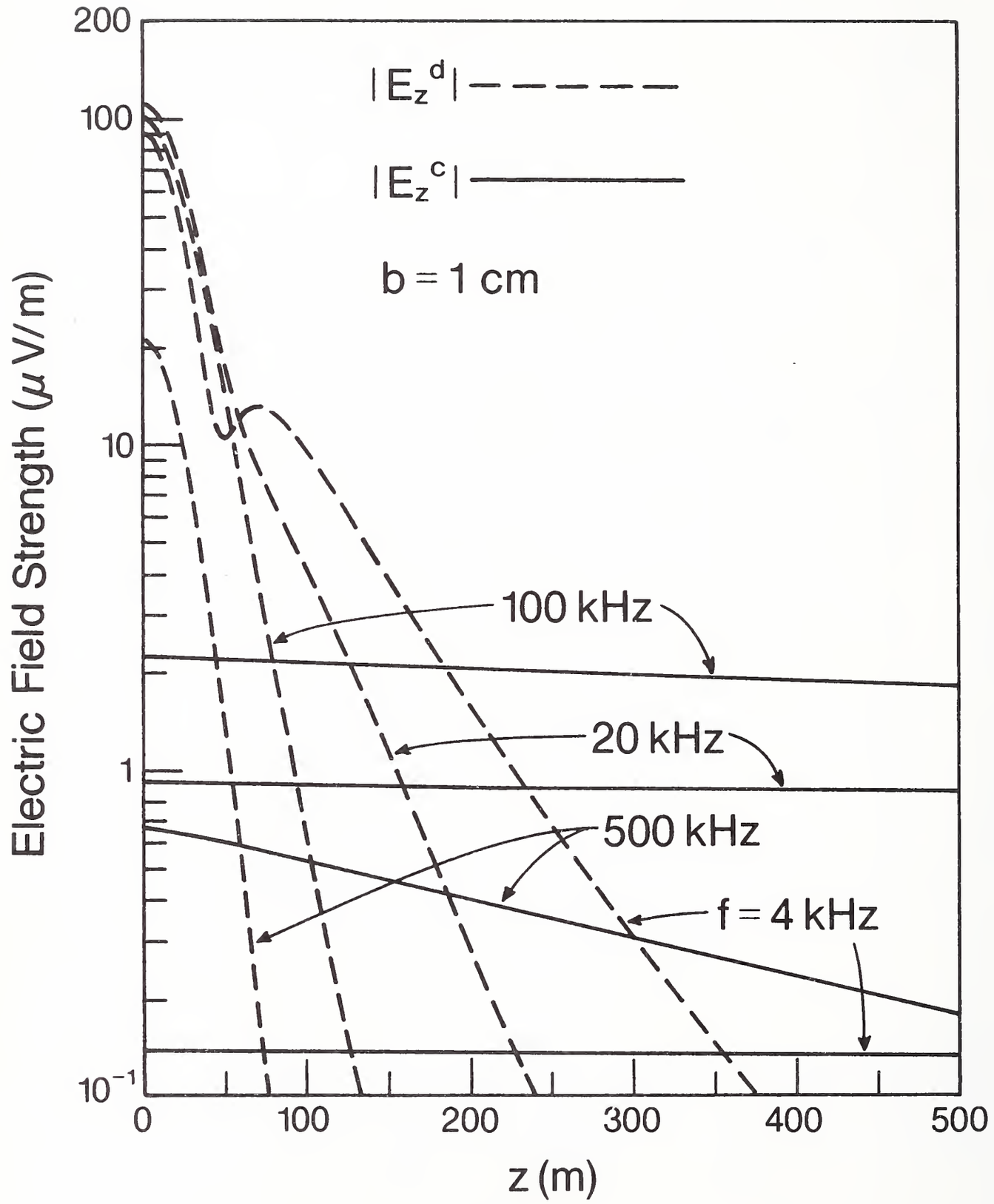

Figure 9. Primary $|E_z^d|$ and secondary $|E_z^c|$ electric field strength for different frequencies.

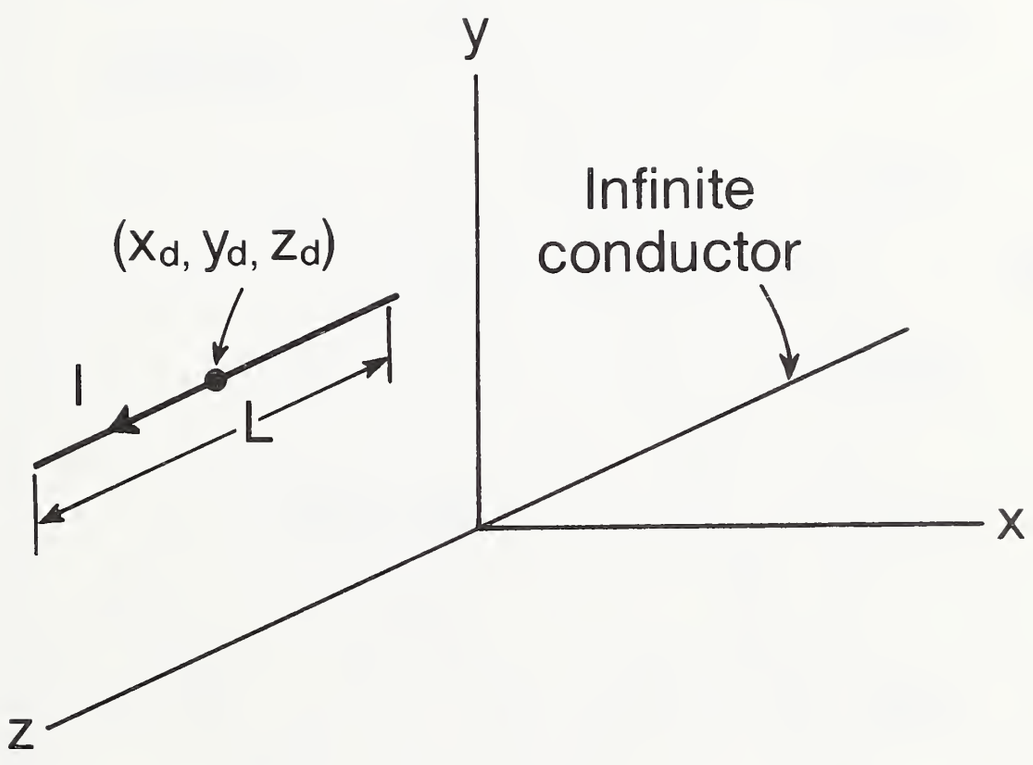

Figure 10. Geometry for a horizontal line source and an infinitely long conductor.

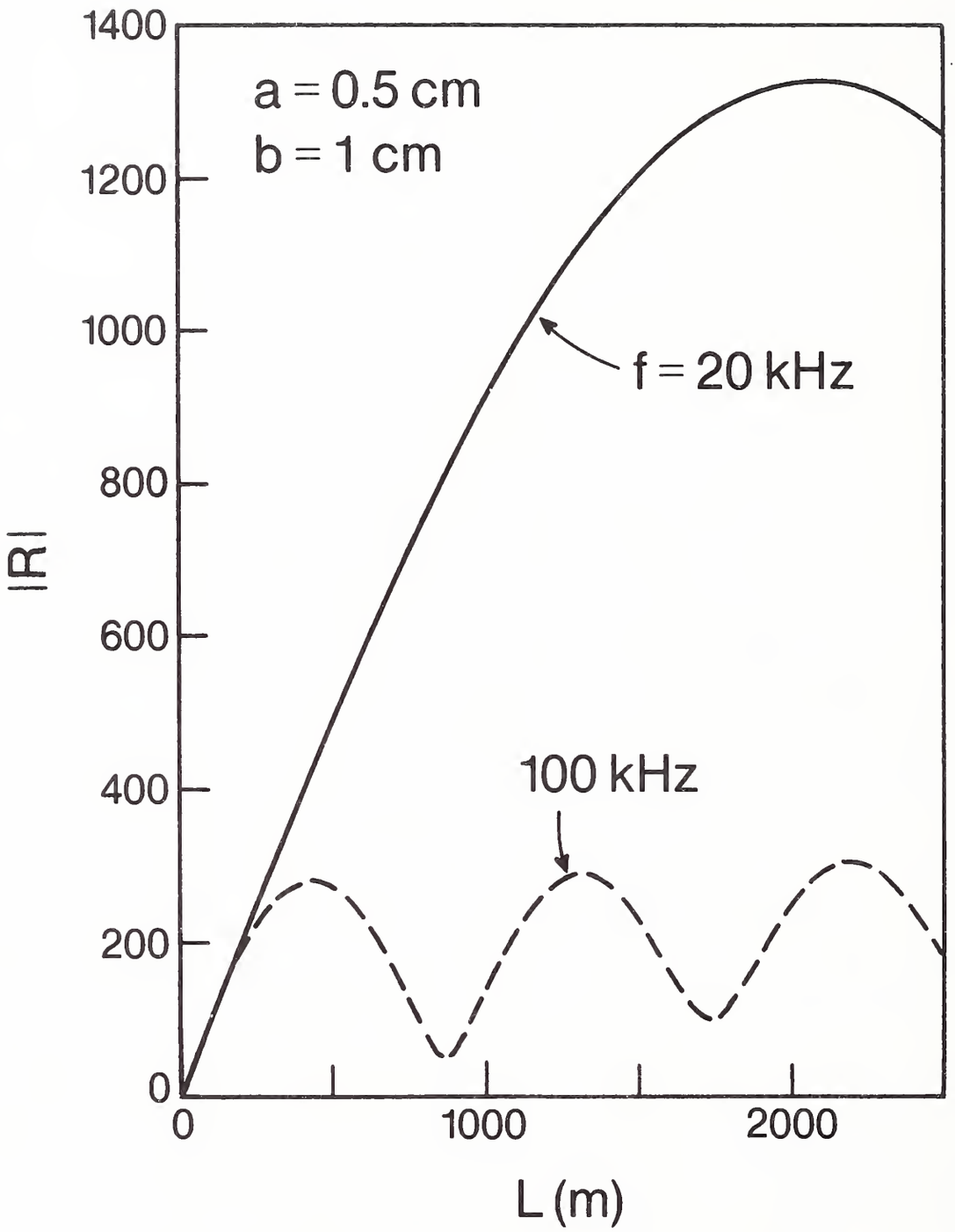

Figure 11. Magnitude of R versus line source length L.

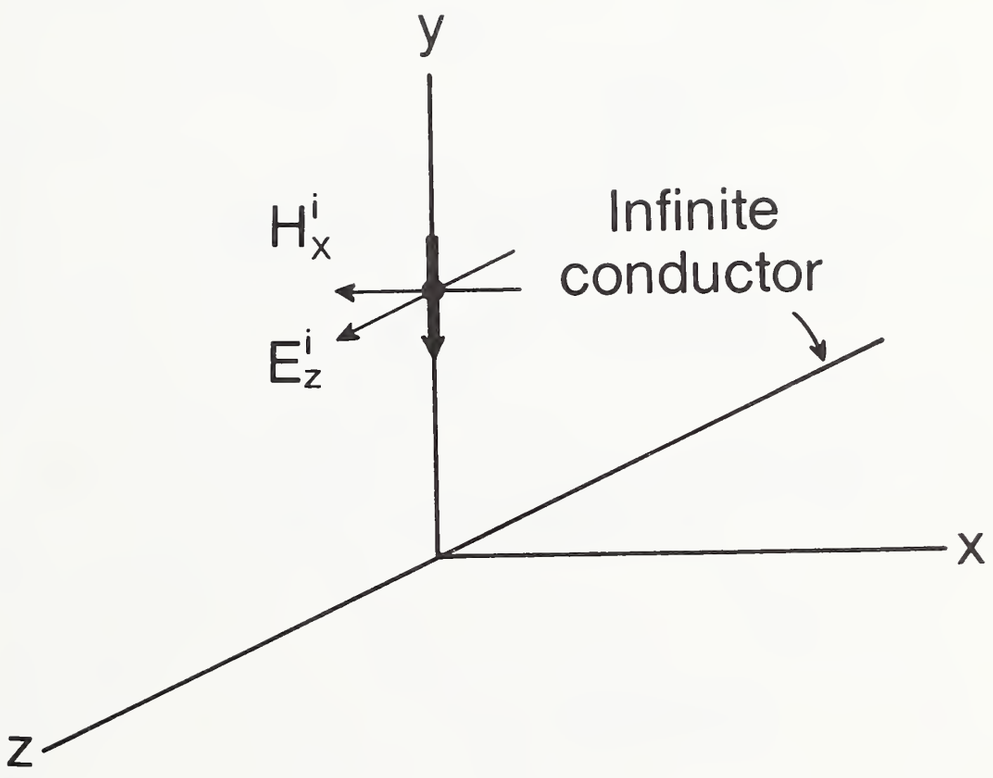

Figure 12. Geometry for a plane wave incident on an infinitely long conductor.

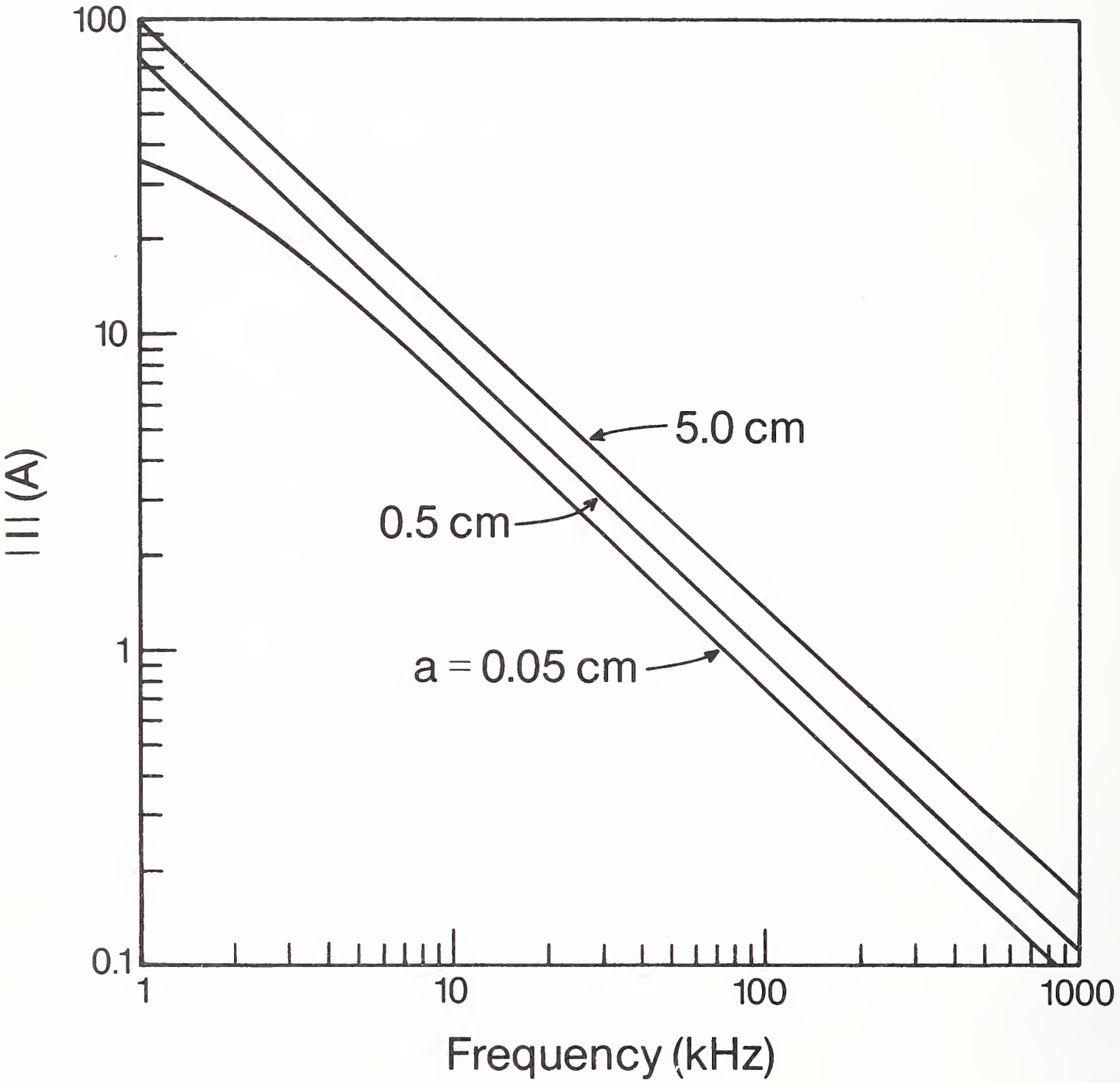

Figure 13. Magnitude of the current induced on an infinitely long conductor for plane wave incidence. E_0 = 1 V/m.

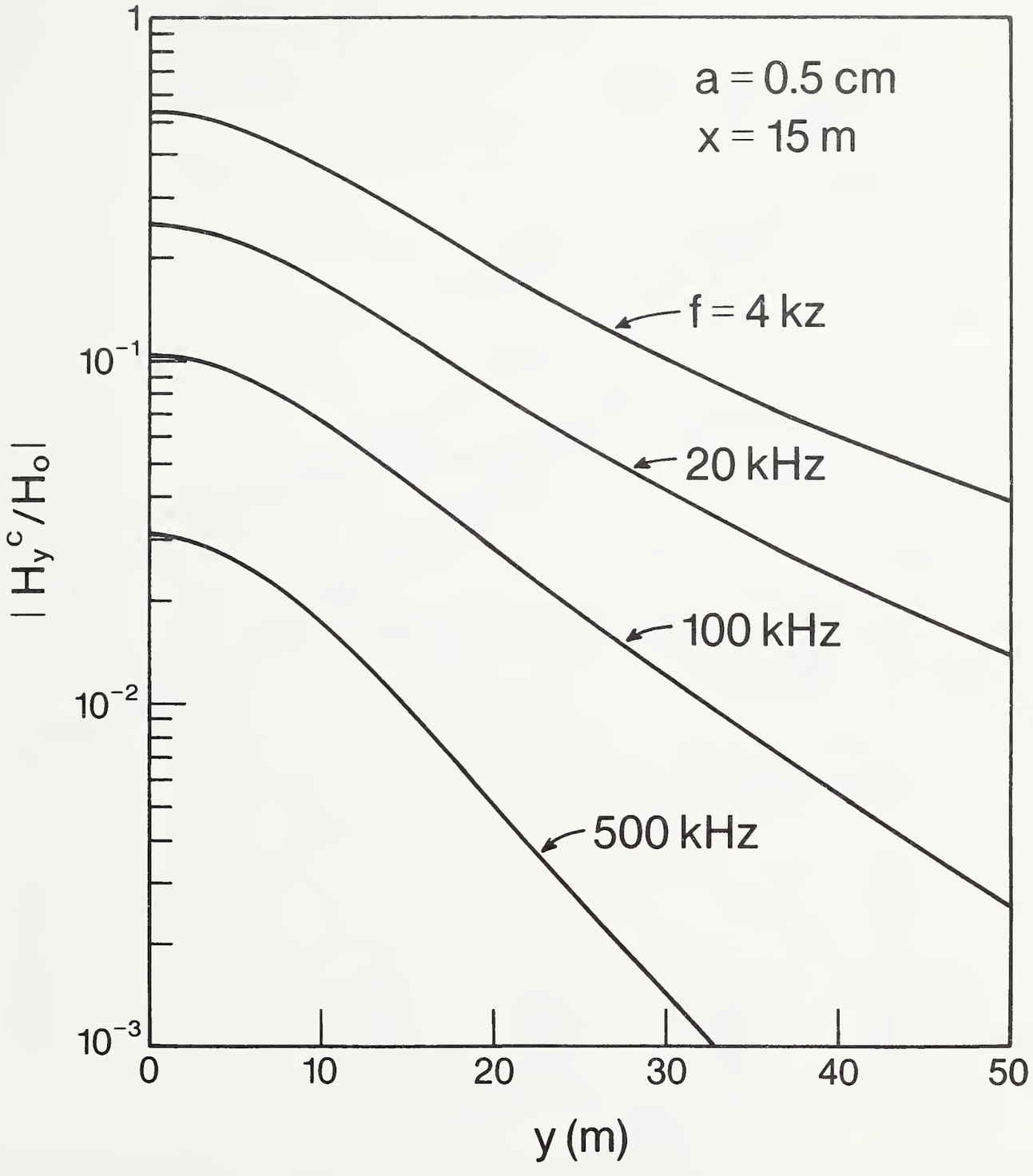

Figure 14. Magnetic field strength for scattering by an infinitely long conductor for plane wave incidence.

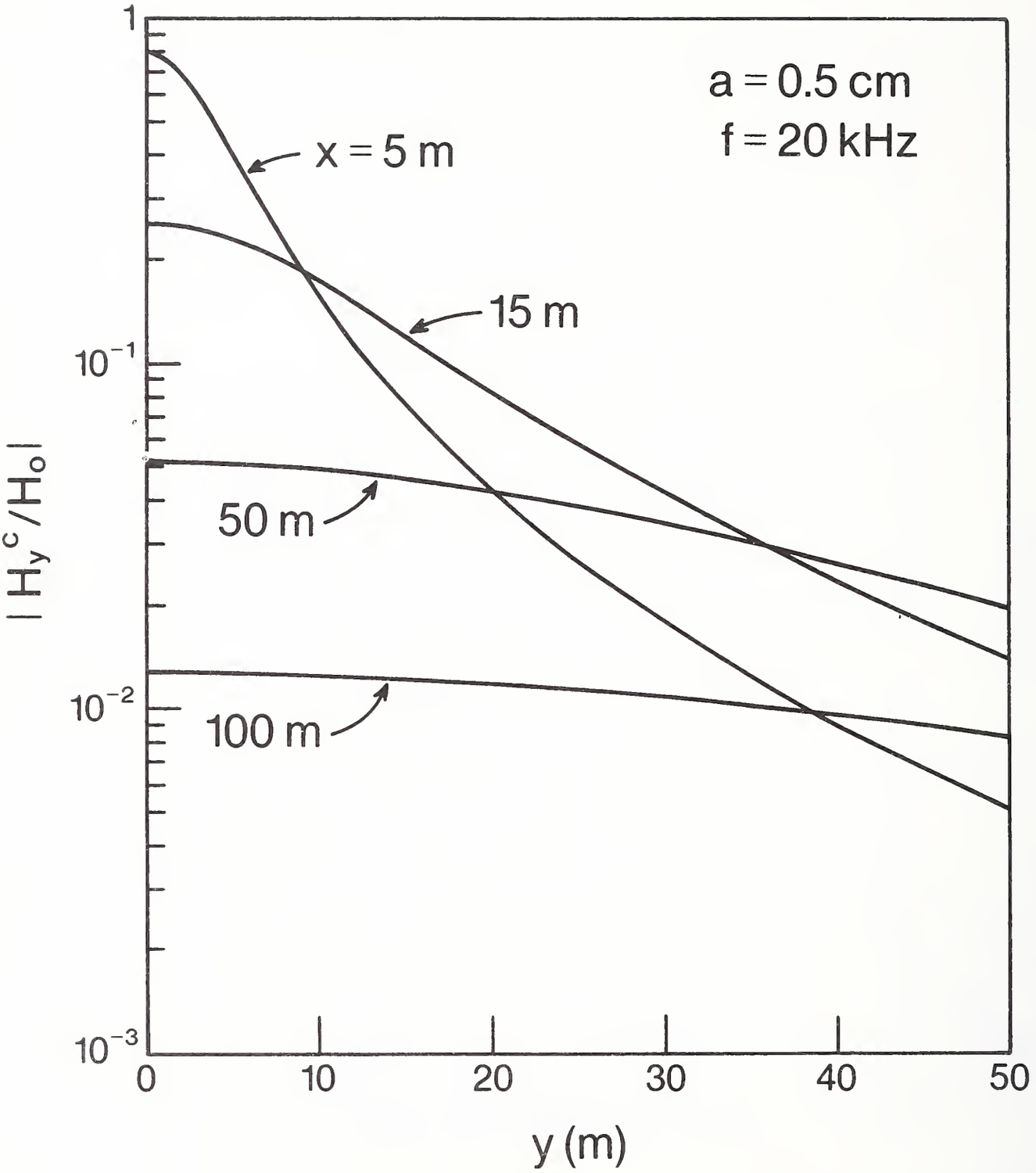

Figure 15. Magnetic field scattered at different horizontal distances x for plane wave incidence.

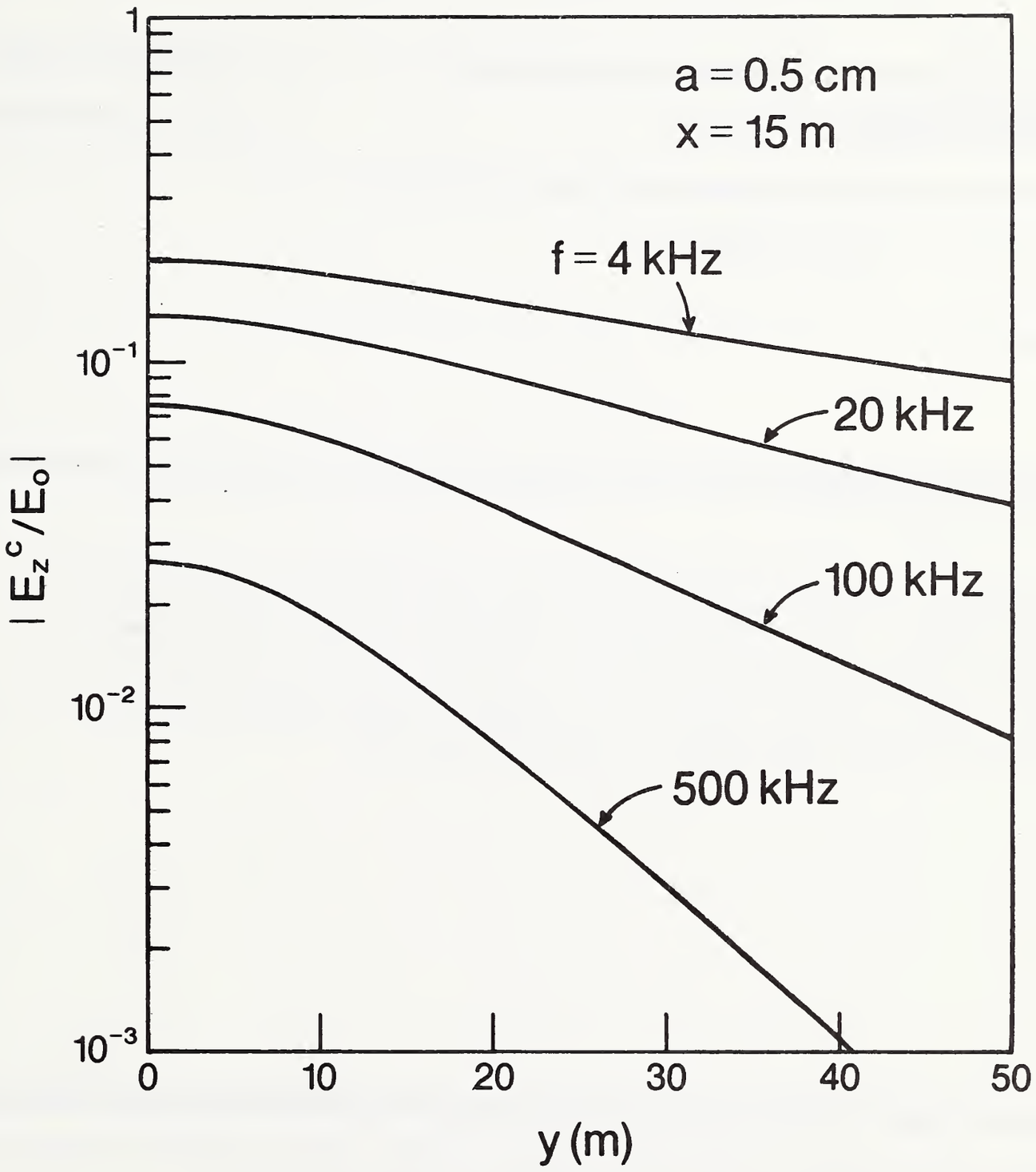

Figure 16. Electric field strength for scattering by an infinitely long conductor for plane wave incidence.

☆U.S. GOVERNMENT PRINTING OFFICE: 1990 - 573-581/45020

L-114A
-90)

U.S. DEPARTMENT OF COMMERCE
NATIONAL INSTITUTE OF STANDARDS AND TECHNOLOGY

BIBLIOGRAPHIC DATA SHEET

1. PUBLICATION OR REPORT NUMBER
NISTIR 3954

2. PERFORMING ORGANIZATION REPORT NUMBER

3. PUBLICATION DATE
September 1990

TITLE AND SUBTITLE

Near-Field and Far-Field Excitation of a Long Conductor in a Lossy Medium

AUTHOR(S)

David A. Hill

PERFORMING ORGANIZATION (IF JOINT OR OTHER THAN NIST, SEE INSTRUCTIONS)

U.S. DEPARTMENT OF COMMERCE
NATIONAL INSTITUTE OF STANDARDS AND TECHNOLOGY
BOULDER, COLORADO 80303-3328

7. CONTRACT/GRANT NUMBER

8. TYPE OF REPORT AND PERIOD COVERED

SPONSORING ORGANIZATION NAME AND COMPLETE ADDRESS (STREET, CITY, STATE, ZIP)

U.S. Army Belvoir RD&E Center
Fort Belvoir, Virginia 22060-5606

). SUPPLEMENTARY NOTES

1. ABSTRACT (A 200-WORD OR LESS FACTUAL SUMMARY OF MOST SIGNIFICANT INFORMATION. IF DOCUMENT INCLUDES A SIGNIFICANT BIBLIOGRAPHY OR LITERATURE SURVEY, MENTION IT HERE.)

Excitation of currents on an infinitely long conductor is analyzed for horizontal electric dipole or line sources and for a plane-wave, far-field source. Any of these sources can excite strong currents which produce strong scattered fields for detection. Numerical results for these sources indicate that long conductors produce a strong anomaly over a broad frequency range. The conductor can be either insulated or bare to model ungrounded or grounded conductors.

12. KEY WORDS (6 TO 12 ENTRIES; ALPHABETICAL ORDER; CAPITALIZE ONLY PROPER NAMES; AND SEPARATE KEY WORDS BY SEMICOLONS)

axial current; axial impedance; electric dipole; electric field; grounded conductor; insulated conductor; line source; magnetic field, plane wave.

13. AVAILABILITY

X	UNLIMITED
	FOR OFFICIAL DISTRIBUTION. DO NOT RELEASE TO NATIONAL TECHNICAL INFORMATION SERVICE (NTIS).
	ORDER FROM SUPERINTENDENT OF DOCUMENTS, U.S. GOVERNMENT PRINTING OFFICE, WASHINGTON, DC 20402.
X	ORDER FROM NATIONAL TECHNICAL INFORMATION SERVICE (NTIS), SPRINGFIELD, VA 22161.

14. NUMBER OF PRINTED PAGES
40

15. PRICE

ELECTRONIC FORM